RSC Advances

ROYAL SOCIETY OF CHEMISTRY

www.rsc.org/advances

Preparation and characterization of exfoliated graphene oxide-L-cystine as an effective adsorbent of Hg(II) adsorption

A. Santhana Krishna Kumar[a], Shiuh-Jen Jiang[a,b]*

[a] Department of Chemistry, National Sun Yat-sen University, Kaohsiung 80424, Taiwan

[b] Department of Medical Laboratory Science and Biotechnology, Kaohsiung Medical University, Kaohsiung 80708, Taiwan. *Corresponding author. Tel: +886-7-312-1101 ext. 2251

E-mail address: sjjiang@mail.nsysu.edu.tw (S.-J. Jiang).

Abstract

A facile and novel method for removal of Hg(II), based on the appealing interaction between exfoliated graphene oxide (EGO), L-cystine, and Hg(II), is reported in this paper. A thiol functional group facilitated the interaction with Hg(II), resulting in an efficient adsorption. The abundant oxygen-containing functional groups on the surfaces of graphene oxide (GO) play an important role in Hg(II) sorption. Characterization of the adsorbent was performed using various characterization techniques, such as cross polarization magic angle spinning nuclear magnetic resonance, Raman spectroscopy, x-ray photoelectron spectroscopy, Powder-X-ray diffraction, Fourier transform infrared spectroscopy, scanning electron microscope and energy-dispersive x-ray analysis. The capability of inductively-coupled plasma mass spectrometry for Hg(II) adsorption was extensively studied under different optimal parameters and the adsorption isotherm values clearly fit with the Langmuir isotherm plot; maximum adsorption capacity was 79.36 mg g^{-1}, augmented by the thermodynamically favourable adsorption process. Second-order kinetics of the adsorption process were validated by the experimental data. Regeneration of the adsorbent was accomplished using thiourea and the potential of this novel adsorbent material was utilized in Hg(II) adsorption.

Introduction

Mercury is considered one of the most toxic heavy metals in both atmospheric and aqueous systems because of its bioaccumulation in the food chain.[1] The most toxic form of mercury is highly reactive Hg^{2+}, which binds to the amino acid cystine in proteins. In contrast, the danger of elemental mercury (Hg^0) and organo-mercury compounds lies in their transport routes; mercury vapor is easily inhaled and enters the blood stream in the human body, while the toxicity of mono methylmercury ($MeHg^+$) or dimethylmercury (Me_2Hg) is caused by their ability to penetrate membranes within fractions.[2, 3] Mercury is well-known for its toxicity even at very low concentrations; the drinking water criterion for mercury, established by US EPA, is 2.0 μgL^{-1}, and the permitted discharge limit of wastewater for total mercury is 10.0 μgL^{-1}.[4,5] Water contamination of mercury arises in various ways, including contamination from electrical and electronics manufacturing plants, chloro-alkali plants, sulfide ore roasting operations, and battery industries.[6] Therefore, removal of mercury in water and wastewater is important for environmental protection, and thus it is necessary to remove mercury contaminants from wastewater before it is released into the environment. Several techniques have been proposed for the treatment of wastewater containing mercury, including are precipitation, coagulation, adsorption, ion exchange, and chemical reduction; among these methods, the most promising process for the removal of metal ions is adsorption. Several adsorbents have been studied for heavy metal removal, but adsorption techniques have been conventionally associated with activated carbon as the adsorbent. However, there is now increasing interest in the development of new selective adsorbents prepared by various chemical modifications.

Therefore, there is a need to develop innovative, low-cost adsorbents useful both for industries and the environment. Graphene and graphene oxide (GO) were used as effective adsorbents of heavy metals. Graphene, as a single atomic layer of sp^2 carbon atoms, has recently attracted tremendous attention within the scientific community due to its unique attributes, such as high conductivity, optical transparency, and mechanical stability.[7] GO has plenty of oxygen atoms on the graphitic backbone, in the forms of epoxy, hydroxyl, and carboxyl groups, which protrude from its layers, and these groups can bind to heavy metals. GO is more useful for adsorption of heavy metals due to the presence of several functional groups on its surface. [8-12] EGO has been suggested as "a superior adsorbent" for excellent sorption of heavy metals; oxidized graphene has shown exceptional adsorption capacity and high adsorption efficiency for metal removal.[13,14] Graphene or GO, products of graphite from an oxidization process, may be ideal materials for wastewater treatment. Normally, graphene obtained from graphite exists in two states, i.e., GO and reduced graphene oxide (RGO). GO is hydrophilic with low conductivity, while RGO is hydrophobic with good conductivity.[15]

Graphene-based materials have potential applications in wastewater treatment,[16,17] and because adsorption is a superficial phenomenon, the surface properties of the adsorbent plays very important role in deciding its sorption ability. Several graphene-based, functionalized adsorbents have been employed to remove Hg(II) from aqueous solution. For example, thiol-functionalized adsorbents exhibited specific binding capability towards Hg(II) due to the thiol (SH) groups[18]; covalent modification of porous materials with complexing groups, such as SH, can significantly increase the adsorption efficiency for Hg(II) removal.[19] Moreover, materials which carry sulfur, nitrogen, and oxygen-containing functional groups as major binding sites are effective for mercury removal.[20] Among the above-mentioned materials, sulfur-containing groups bind more

effectively, due to soft−soft interaction with the Hg(II). Therefore, it can be presumed that a sulfur ligand-functionalized EGO may be an apt option for efficient removal of Hg(II). However, graphene has huge potential for sensors; application of amino acid-modified GO was used as a electrochemical sensor for Hg(II) detection.[21,22]

In this work, the functionalization of L-cystine onto EGO for Hg(II) adsorption have not been explored, despite that L-cystine is a well-known complexing agent able to bind soft metal ions in aqueous solution. The L-cystine bears an amino group ($-NH_2$) that could interact with EGO hydroxyl and carboxyl groups through covalent bond interaction, and the same material has been used for heavy metal detection, as reported recently.[23] Furthermore, L-cystine is well-investigated for Hg(II) adsorption in the present work.

Experimental

Preparation of exfoliated graphene oxide from graphite

An improved method was used for the synthesis of GO, which was reported in earlier studies.[24,25] About 1.5 g of graphite powder was taken and gradually added to a 9:1 mixture of concentrated H_2SO_4/H_3PO_4 (180:20 mL). The reaction was slightly exothermic to 35-40 ^{0}C, after which it was heated up to 60 ^{0}C with continuous stirring for 12h. The above reaction mixture was cooled to room temperature and slowly poured onto ice (200 ml) with 2 ml of H_2O_2 (30%) where the brown color was entirely turned to yellow. Afterwards, centrifugation of the filtrate was done at 4500 rpm for 30 minutes and the supernatant was decanted. The solid material obtained after centrifugation was thoroughly washed with 200 ml of water followed by 200 ml of 30% HCl and 200 ml of ethanol. After each wash, the filtrate was centrifuged at 4500 rpm for 30 minutes and the supernatant was decanted off. The leftover solid material was dried at room temperature for 12 hours. 1.0 g of EGO was dispersed in 50 mL of a thionyl chloride ($SOCl_2$)–

dimethylformamide (DMF) solution. The resulting mixture was refluxed at 70^0C for 24 hours and then centrifuged several times to isolate the precipitate. The isolated precipitate was washed with tetrahydrofuran (THF) and dried under vacuum.[26]

Preparation of adsorbent

1g of EGO was taken in a round-bottom flask followed by slow, drop-wise addition of 0.004 molar of L-cystine, which dissolved in acetone medium and was stirred up to 10 hours at room temperature. The resulting mixture was washed thoroughly with acetone and filtered. The un-reacted L-cystine was removed by repeated washing with acetone. The solid was dried at room temperature overnight and used for further adsorption studies. Comprehensive characterization of the adsorbent was done using various physico-chemical techniques to confirm the presence of L-cystine and EGO in the adsorbent.[27]

Batch adsorption study

Batch adsorption isotherm studies were carried out with varying concentrations of Hg(II) solution. 0.15 g of the L-cystine-EGO adsorbent were taken for analysis in an aqueous phase volume of 30 mL of Hg(II). At optimum pH (5.5 to 7.0), the amount of Hg(II) adsorbed (q_e) was obtained by equilibration at various concentrations using the expression q_e:

$$q_e = \frac{(C_o - C_e)\, V}{W} \qquad (1)$$

where C_o and C_e indicate the initial and equilibrium Hg(II) concentrations, respectively, and V and W specify the volume of sample solution (L) and the weight (g) of the L-cystine-EGO adsorbent, respectively. The supernatant was collected for further ICP-MS analysis to determine the Hg(II) concentration after adsorption (Table T1 of supporting information ESI†).[28]

Results and discussion

Raman spectrum

The Raman spectrum graphite shows a *D* peak at 1350 cm^{-1} (D band) of crystalline graphite, alternating ring stretch vibration in condensed benzene rings and a very strong peak at 1575 cm^{-1} (G band) sp^2 stretch vibration in benzene or condensed benzene rings, C=C sp^2 stretch vibration of olefinic/conjugated chains, a 2441 cm^{-1} D' band, and a 2D band at 2701cm^{-1} (Fig. 1A). EGO shows a D band at 1360 cm^{-1} , G bands at 1601 cm^{-1} and a D' band at 2443 cm^{-1} (Fig. 1B). However, in EGO, the D and G bands have equal intensity, confirming that graphite completely oxidized to GO. Thus, the integrated intensity ratio of the D and G-bands (I_D/I_G) indicates the oxidation of graphite to EGO and the size of the sp^2 ring clusters in a network of sp^3 and sp^2 bonded carbon. After oxidation to EGO, the intensity of the I_D/I_G ratio increased from 0.52 to 0.99, implying that the reduced state increases the number of aromatic domains, thus leading to an increase in the I_D/I_G ratio; this phenomenon was interpreted in earlier studies.[26]

Powder XRD pattern

The powder XRD patterns (Fig. 2) of graphite show a very sharp diffraction peak for graphite at $2\theta = 26.28^0$ (d = 0.33 nm) corresponding to the plane (002), which shifts to 10.46^0 (d = 0.84 nm) on chemical oxidation, indicating the formation of EGO. The C-axis spacing increases from 0.33 to 0.84 nm after oxidation from graphite to GO, due to the creation of the abundant oxygen-containing functional groups on the surfaces of GO.[29]

Solid state NMR

Cross-polarization, magic-angle spinning nuclear magnetic resonance spectroscopy (^{13}CPMAS-NMR) is the most powerful method available to study the detailed chemical structures of graphene-based materials such as EGO. Typical solid-state ^{13}CPMAS-NMR spectra reveal that there are two main peaks in the ^{13}CPMAS-NMR spectrum of EGO. The peak at 61 ppm is

assigned to carbon atoms bonding to the epoxy group and the peak at 132 ppm is ascribed to the graphitic sp^2 carbon (Fig. 3). In addition, high-resolution ^{13}CPMAS-NMR spectra revealed another three small peaks that were found at about 97.8, 167, and 188 ppm.[19] These three weak peaks were tentatively assigned to lactol, ester carbonyl, and ketone groups, respectively.

UV-Visible spectroscopy

EGO gives distinct characteristic peaks observed at 234 nm (corresponding to π-π* transitions of C=C bonds) and 300 nm (due to n-π* transitions of COOH groups) (Fig. 4). The overall feature of this spectrum is identical to EGO synthesised using the conventional improved Hummers synthesis of graphene method and the peaks are also similar to those earlier reported in the literature[30]; the dispersion of EGO shows a clear yellow colour, indicating a successful oxidation of graphite to EGO.

FT-IR spectral analysis

The distinct pure graphite peaks in the Fourier transform infrared spectroscopy (FT-IR) spectrum corresponded to aromatic C-H stretching at 3412 cm^{-1}, C=C stretching 1638 cm^{-1}, C-H bending at 1536 &1440 cm^{-1}, C-C stretching at 1133 cm^{-1} (Fig. 5A), and the peaks at 616 and 724 cm^{-1} originated from the phenyl ring in pure graphite.[17] After oxidation with the improved synthesis, GO has several functional groups that were introduced, such as hydroxyl, carboxylic acid, and epoxy groups. EGO shows a broad peak at 3408 cm^{-1}, which refers to the O-H stretching of the hydroxyl group[31] (Fig. 5B), which can be ascribed to the oscillation of carboxyl groups. The FT-IR spectra of oxidized EGO shows four major peaks, located at 3715, 3408, 2303, and 1564 cm^{-1}, respectively. The peak at 3715 cm^{-1} is attributed to free hydroxyl groups. The peak at 3408 cm^{-1} can be assigned to the O-H stretch from carboxyl groups (O=C−OH and C−OH), while the peak at 2303 cm^{-1} can be associated with the O−H stretch from strongly hydrogen-bonded COOH.[32] The peak at 1564 cm^{-1} is related to the carboxylate anion stretch mode.[33] The peak at

1638 cm^{-1} can be associated with the stretching of the EGO backbone.[34] The carbonyl group (C=O) stretching vibrations appeared in a new peak at 1705 cm^{-1}. Increased strength of the signal at 1193 cm^{-1} may be associated with C–O stretching in the same functionalities.[35] The peaks at around 2804 and 2696 cm^{-1} correspond to the C-H stretch modes of H−C=O in the carboxyl group.

After functionalization with L-cystine, three new, characteristic peaks were found: the 1336 cm^{-1} peak corresponded to C=N stretching, N-CS stretching was at 1086 cm^{-1}, and C-S stretching was at 969 cm^{-1}.[36] The OH peaks indicate a relatively free hydroxyl group in EGO and a carboxyl group, both of which involve functionalization with L-cystine (Fig. 5F), which involves inter- and intra-molecular hydrogen bonding. However, in this case of EGO functionalization with L-cystine, it can be observed that the NH_2 peak has shifted to a lower value and the intensity of the amino group NH-CO (amide I) has decreased, which proves that NH_2 groups on the L-cystine chains reacted with the COOH groups onto the surface of EGO and therefore were converted to NHCO graft points.[37] After Hg(II) adsorption onto the adsorbent, the ligand is bonded through the sulphur, as indicated from the observed shift (C-S) vibration from 611 cm^{-1} to a lower wave number with the simultaneous appearance of a new band at 415cm^{-1}, due to (Hg-S).[35,38] Deprotonation of the enolic OH of the reagent in the complex formation was also confirmed by the disappearance of OH and the appearance of Hg-O at 549 cm^{-1}, providing an additional support for the oxime oxygen donation. Similar strong effects were also derived for other peaks (N-H vibrations) at 1638 and 1580 cm^{-1} (Fig. 5G). The presence of Hg(II) produces a broader, sharp peak at 1580 cm^{-1} and a strong intensity increase[39] in the peaks at 1197 and 1092 cm^{-1}.

EDX analysis

The energy-dispersive x-ray analysis (EDX) spectrum, after adsorption of Hg(II) on to the adsorbent, had characteristic peaks (1-3 keV), confirming the presence of adsorbed Hg(II) along with other elements, such as carbon, oxygen, and sulphur (Fig. S1 of Supporting Information ESI†).[40]

X-ray photoelectron spectroscopy analysis

The x-ray photoelectron spectroscopy (XPS) studies of the L-cystine–EGO novel adsorbent after the Hg(II) adsorption experiment show the presence of Hg(II), carbon, nitrogen, sulphur and oxygen (Fig. 6A). The C1s spectrum (Fig. 6B) shows that C–C (284.7 eV) and C(O)O (288.3 eV) peaks from carbon bound with oxygen.[20] The N1s spectrum (Fig. 6C) was assigned to peak at the binding energies of 401.5 eV for the NH_2 group that interacted with the EGO/L-cystine adsorbent. The oxygen 1s spectrum (Fig. 6E) can be assigned a peak at 531.1eV, which represents the binding energies of oxygen. The XPS spectra of EGO-L-cystine shows a peak at 161.8 eV (Fig. 6F) as for $S2p_{3/2}$ in standard L-cystine,[26, 41] confirming the SH-group of the L-cystine onto the surface of adsorbent after adsorption of Hg(II) onto the adsorbent.[42]

Deconvolution of Hg4f shows two peaks at 100.5 eV and 104.6 eV (Fig. 6D), indicative of Hg(II) adsorption onto the surface of the adsorbent, which has a spin–orbit splitting of 4.1 eV for the $4f_{7/2}$ and $4f_{5/2}$ states.[20] In the N1s spectrum after Hg(II) adsorption, it is possible to observe that some of the nitrogen sites are free (constant BE) whilst others contributed to a charge transfer from amino sites to Hg(II). The Hg(II) adsorption is followed by the appearance of a doublet (Hg $4f_{5/2}$ and $4f_{7/2}$) with symmetric peaks. The BEs of Hg $4f_{7/2}$ of the most appropriate reference compounds are 100.5 eV for $HgCl_2$ and 104.6 eV for HgO; for L-cystine-EGO, it is possible to assume that the adsorbed mercury species are in $HgCl_2$ form and HgO would be possible. Again, the L-cystine-EGO adsorbent shows a mechanism of adsorption that would

present more free amino groups. Sulphur present in L-cystine is a more soft basic ligand then amino or hydroxyl groups, and these ligands could interact with a soft acid such as Hg(II); this fact can explain the high adsorption capacity of L-cystine-EGO for Hg(II), compared to earlier studies.

Effect of pH

The effect of pH on the adsorption of Hg(II) by L-cystine-EGO was studied by varying pH over a range of 1 to 10 using 0.1 N NaOH/HCl. The nitrogen atom of the amino group, oxygen atoms of the hydroxyl groups, and sulphur atoms of L-cystine chelating ligands can bind a metal ion by electron pair-sharing to form a metal chelate-complex. Because of the stronger attraction of the lone pair of electrons to the nucleus in an oxygen atom than in a nitrogen atom, the nitrogen atoms have a greater tendency to donate the lone pair of electrons for sharing with a metal ion to form a metal complex than the oxygen atoms. The higher electronegativity of oxygen compared to nitrogen and sulphur (electronegativity increasing in the order S < N < O) indicates that the donation of a lone pair of electrons from the nitrogen and sulphur atom will be more facile than the oxygen atom for bond formation with Hg(II).[43,44] In the case of L-cystine-EGO under highly acidic conditions (pH 1 to 4.5), there was less sorption of Hg(II) because of the chloro complex of Hg(II) and competition between monovalent protons (H^+) for binding sites.[45] As you see here, the predominant species between pH 1 to 5.0 is mercury, as $HgCl_2$(aq); when the pH, decreases Cl concentration increases as a result of very stable Hg(II) chloride complexes, namely $HgCl_3^-$ (aq) and $HgCl_4^{2-}$ (aq), which become predominant in aqueous medium. Therefore, under these conditions, there is a true competition between the formations of the Hg(II)-sulfur bond.[46] At highly basic pH, the sorption of Hg(II) decreases because of the competition of hydroxide ions (OH^-); the optimum pH is 5.5 to 7, thus mercury would be neutral, existing as divalent mercury,

until it's ready to accept a lone pair of electrons from sulphur, oxygen, or nitrogen atoms, which generates the surface complexation[45] (Fig. S2A of supporting information ESI†).

Adsorption mechanism

The adsorption of Hg(II) onto the adsorbent can be defined as physical adsorption, chemical adsorption, and electrostatic attraction; chemical adsorption and electrostatic attraction are major factors that can affect the adsorption performance of an adsorbent. The pH of the aqueous medium plays an important role in the interaction of Hg(II). At low pH range (1-5), mercury forms $HgCl_2$ and $HgCl^+$; when the pH decreases to values lower than 5.0, the HCl concentration increases as Hg(II) chloride complexes,[46-48] as $HgCl_3^-$(aq) and $HgCl_4^{2-}$(aq) predominate.[46,49] The optimum pH for adsorption of Hg(II) onto L-cystine-functionalized EGO adsorbent was observed in the range of pH 5.5 to 7. We hypothesized that Hg(II) is bound to L-cystine functionalized with EGO adsorbent, which presented SH, amino ($-NH_2$), OH, and COOH functional groups containing oxygen, nitrogen and sulphur. The excellent ability of Hg(II) to behave as a typical soft acid is well-suited to interact with ligands containing sulphur, oxygen and nitrogen as the heteroatom. According to the Pearson's concept, Hg(II), being a typical soft acid, has the ability to coordinate with sulphur, oxygen, and nitrogen to form a stable metal chelate-complex. The L-cystine amino group would involve in covalent interaction with the surface hydroxyl and carboxyl groups onto the surface of EGO; furthermore, L-cystine electron donor groups like the amino, oxygen, and sulphur groups, donate electrons to Hg(II) which generates surface complexation. The overall mechanism that could be conceptualized in this adsorption process is given in Fig. 7. A highly basic pH value decreases the concentration of $HgCl_2$ while increasing that of $Hg(OH)_2$; with increases in pH, the repulsion of the negatively-charged EGO surface (due to the deprotonation of the surface hydroxyl groups, carboxyl group, and amino group) and the formation of $Hg(OH)_2$ species[50] lead to a reduction in percentage

adsorption. At highly alkaline pH, the sorption of Hg(II) decreases because of competition from hydroxide ions.

Amount of adsorbent

In the batch experiments, the amount of the adsorbent material varied in the range of 0.05 to 0.25g. The amount of Hg(II) adsorbed onto L-cystine-EGO was found to be maximium (99 %) in the range of 0.15 to 0.2g in a 30 mL sample volume. The available adsorption sites and surface area increase by varying the adsorbent dosage; therefore, the results reveal an increase in the percentage adsorption of Hg(II). Although the percentage adsorption increases with adsorbent dose, the amount of Hg(II) adsorbed per unit mass decreases. This is supported from the trend in % adsorption of Hg(II), which shows a sharp increase initially and later attains its maximum at 0.15g of the adsorbent (Fig. S2B of supporting information ESI†). The decrease in % adsorption of Hg(II) with an increase in adsorbent dose is attributed to desaturation of adsorption sites in the process of adsorption.

Adsorption isotherm Langmuir isotherm

The Langmuir adsorption isotherm is based on the fact that adsorption is homogeneous with monolayer coverage. The isotherm assumes that all sites are equivalent and have uniform surface coverage. The Langmuir isotherm model,[51] with equivalent sites and linear form, can be expressed as

$$\frac{C_e}{q_e} = \frac{1}{q_o b} + \frac{C_e}{q_o} \qquad (2)$$

'q_o' and 'b' are the Langmuir constants related to the adsorption capacity and intensity, respectively. A plot of C_e/q_e vs C_e gives the q_o and b (Fig. S3A of supporting information ESI†),

and the feasibility of the adsorption process is determined by R_L (which is dimensionless), known as the separation factor, which is given as

$$R_L = \frac{1}{1 + bC_o} \qquad (3)$$

The R_L value has considerable importance when it is between 0 and 1, where it implies an effective interaction between the adsorbent and the adsorbate. Values greater than 1 are an indication of an unfavorable isotherm, and R_L equal to zero is accounted for a totally irreversible isotherm; these features are summarized in TableT2 of the supporting information (ESI†). The Langmuir isotherm parameters, and a relatively good regression coefficient (TableT3 of supporting information ESI†), indicate the effectiveness of interaction between the Hg(II) and the L-cystine-EGO adsorbent.

Freundlich isotherm

The Freundlich isotherm[52] yields the constants K_F and n (TableT3 of supporting information ESI†), reflecting the adsorption capacity and intensity, respectively. The Freundlich adsorption equation can be expressed as

$$\log q_e = \log K_F + \frac{1}{n} \log C_e \qquad (4)$$

These constants are easily obtained from the log-log plots of q_e against C_e (Fig. S3B of supporting information ESI†). K_F and n are the Freundlich constants that indicate the adsorption capacity and the adsorption intensity, respectively; a favorable adsorption would have a Freundlich constant n between 1 and 10. A higher value of n (smaller value of 1/n) implies effective interaction between the adsorbent and adsorbate (TableT3 of supporting information

ESI†). When $1/n < 1$, it corresponds to a normal L-type isotherm, while $1/n > 1$ reflects a co-operative sorption.[17]

Adsorption kinetics

Pseudo-first-order kinetics

The first-order rate expression of Lagergren [53] can be expressed mathematically as

$$\log (q_e - q_t) = \log q_e - \frac{k_1 t}{2.303} \qquad (5)$$

These equations relate the amount of Hg(II) adsorbed onto the L-cystine-EGO adsorbent and the rate constants at varying time intervals, where q_e and q_t (mgg^{-1}) are the amounts of Hg(II) adsorbed per unit mass of adsorbent at equilibrium and time in min, respectively, and k_1 is the rate constant. The values of the adsorption rate constant (k_1) for the sorbents at different initial Hg(II) concentrations were obtained from slopes of the plots of log (q_e-q_t) vs time (Fig. S4A of supporting information ESI†).

Pseudo-second-order kinetics

A pseudo-second-order reaction model[54] utilized in the study of adsorption can be expressed mathematically as:

$$\frac{t}{q_t} = \frac{1}{k_2 q_e^2} + \frac{t}{q_e} \qquad (6)$$

The t/q_t versus t plot (Fig. S4B of supporting information ESI†) in the second-order model gave a nice fit to the experimental data in terms of the higher regression coefficient (Table T4 of supporting information ESI†). The q_e(calculated) and the q_e(experimental) values were in accordance with the second-order kinetics; these values were found to be 2.02 mg g^{-1} and 1.98

mg g^{-1}, respectively. This proximity in the values (Table T4 of supporting information ESI†) further confirms the suitability of the second-order kinetics to the adsorption data.

Intraparticle diffusion

The Weber-Morris model is used to study the intra-particle diffusion and this relates the amount of Hg(II) adsorbed against the square root of time:[55,56]

$$q_t = k_{int}\sqrt{t} + C \qquad (7)$$

where k_{int} is the intra-particle diffusion constant and q_t is the amount of Hg(II) adsorbed at time t. A linear plot of q_t vs $\sqrt{t}$ with a non-zero intercept (Fig. S4C of supporting information ESI†) signifies that the intraparticle diffusion is not the only rate-limiting step. In addition, the Weber-Morris plot does not pass through the origin and hence we can conclude that, in addition to intraparticle diffusion, the boundary layer effect could also influence the kinetics of the adsorption of the Hg(II) into the interlayer of the GO sheets.

Adsorption thermodynamics

The thermodynamics study is an important parameter in order to ascertain the feasibility and nature of the adsorption process. The thermodynamic parameters, namely standard free energy (ΔG^0), standard enthalpy (ΔH^0), and standard entropy (ΔS^0), changed and these changes were determined at various temperature ranges. From thermodynamic studies, the values of the equilibrium constants, ΔH^0 and ΔS^0, were obtained from the slope and intercept of the van't Hoff plot of lnK against 1/T (Fig. S4D of supporting information ESI†). For an exothermic reaction, the slope is positive and the equilibrium constant decreases with increases in temperature: [17]

$$\Delta G^0 = -RT\ \ln K \qquad (8)$$

$$\ln K = \frac{-\Delta H^0}{RT} + \frac{\Delta S^0}{R} \qquad (9)$$

Where is R is the gas constant (J K^{-1} mol^{-1}), T is the temperature in Kelvin, and K is obtained from the ratio of the concentration of Hg(II) in the solid and liquid phases, respectively. The adsorption of Hg(II) was more favourable at room temperature and adsorption gradually decreases at higher temperature; these results reveal that the adsorbate–adsorbent interaction weakened at higher temperatures, indicating that higher temperature is not favourable for the adsorption process. Adsorption is favourable at 300 K, rather than the higher temperatures (Table T5 of supporting information ESI†). The free energy values decreased with rises in temperature; negative free energy is a good indication of spontaneous adsorption. The enthalpy change (ΔH^0) was found to be negative, indicating the exothermic nature of adsorption (Table T5 of supporting information ESI†). The entropy of adsorption (ΔS^0) was also negative; this is indicative of decreased randomness at the adsorbent-solution interface. These facts demonstrate the efficacy of the adsorbent material as a useful material for Hg(II) adsorption.

Column studies

Effect of sample volume

The sample breakthrough volume was ascertained from column study with 1 mg L^{-1} Hg(II), a flow rate of 8 ml min^{-1}, and a sample volume of 400 ml (Fig. S5A of supporting information ESI†) that could be quantitatively adsorbed onto a glass column (1 cm packing height, 30 cm length, 1.0 g L-cystine-EGO adsorbent). The percentage adsorption of Hg(II) decreased at sample volumes above 400 ml; the decrease in percentage adsorption could be ascribed to decreased adsorbent-adsorbate interaction. Thiourea is an effective eluent for Hg(II) and, in the present study, the L-cystine-EGO adsorbent could be regenerated with the above reagent; as low

as 10 ppb of Hg(II) could be adsorbed effectively in the column. Furthermore, the adsorption is also quantitative at an optimized flow rate of 8 mL min^{-1}, which ensures effective contact between the Hg(II) and the adsorbent. The performance of an adsorbent is also expressed in terms of the rate at which the adsorbent bed gets exhausted, the rate of which is given by the ratio of the mass of adsorbent to maximum sample volume.[17] On a laboratory scale, with 1g of the adsorbent, at 1.0 mg L^{-1} Hg(II), the exhaustion rate of the adsorbent is 2.5 g L^{-1}. A lower exhaustion rate signifies the effectiveness of the adsorbent column. Hence, it is possible that, on an industrial scale, with an increase in the amount of the adsorbent in the column, the upper limit for the sample volume would be enhanced correspondingly.

Regeneration and recycle of the adsorbent

The regeneration of adsorbent is an important aspect to be examined in an adsorption process; considering this vital factor, reagents such as thiourea, potassium iodide, potassium bromide, EDTA, DTPA, HNO_3, NaOH, and potassium chloride were examined for effective desorption of Hg(II). Potassium iodide and bromide were tried as eluents because mercury is known to form stable tetraiodo and tetrabromo complexes that could be effectively eluted into the aqueous phase. Thiourea, DTPA, and EDTA are known for their ability to complex Hg(II) through the heteroatoms sulfur, nitrogen, and oxygen. Since Hg^{2+} is a typical soft acid, it has very good affinity towards sulphur-containing ligands like thiourea[46] (Fig. S5B of supporting information ESI†). The order of elution with the above reagents were found to be: thiourea (93%) > potassium iodide (80.9%) > EDTA (37%) > potassium bromide (29.1%) > DTPA (29.0%) > HNO_3 (29.0%) > NaOH (15.0%) > potassium chloride (11.8 %). However, in the proposed methodology, we found that 30 mL of 2.0 mol L^{-1} thiourea was effective for quantitative desorption of Hg(II) in the eluate. In order to regenerate the adsorbent material, an elution step was carried out after each adsorption cycle, when the adsorbent was saturated. The effective

operation of the next sorption process is clearly related to the efficiency of the preceded desorption step. After each elution operation, the adsorbent was washed with deionised water in order to eliminate the remaining thiourea in the adsorbent, and we used 0.1 N NaOH/HCL solution to bring pH above 5.5 for subsequent adsorption studies. We carried out 7 adsorption-desorption cycles and found that the adsorbent is stable and retained its performance efficiency for 4 cycles (99.0%); the data are presented in Fig. S5C of the supporting information (ESI†). The adsorbent could be reused for 4 adsorption-desorption cycles without any noticeable decrease in performance efficiency. Beyond 4 cycles, the available active sites in the adsorbent get saturated and are not readily available for subsequent adsorption studies due to gradually-decreasing adsorption efficiency. However, after 4 cycles, the percentage adsorption of Hg(II) decreases, which could be ascribed to thiourea weakening the interaction between Hg(II) and the adsorbent. Thiourea forms a 1:2 chelate complex with Hg(II), thereby bringing the Hg(II) to the aqueous phase and regenerating the adsorbent.

Effect of foreign ions

The presence of various ions other than Hg(II) may influence the adsorption of Hg(II) ions due to: (i) competition between Hg(II) ions and other ions for adsorption sites; (ii) the complex formation of Hg(II) ions with certain anions; and (iii) the formation of insoluble compounds (i.e. precipitation). In order to evaluate the selectivity of adsorbents towards Hg(II) ions, the extraction of Hg(II) ions was carried out in the presence of several cations and anions.

Effect of cations

In order to probe the degree of Hg(II) selectivity, sorption experiments were carried out in the presence of potentially-contaminating foreign metal ions, such as Cd^{2+}, Co^{2+}, Cu^{2+}, Ni^{2+}, Pb^{2+}, Se^{2+}, Zn^{2+}, and Au^{+}. In these experiments, binary solutions of Hg(II) with the foreign metal ions were used for adsorption of Hg(II) and other accompanying metal ions were investigated (Table

T6 of supporting information ESI†). The presence of foreign ions did not affect Hg(II) sorption at lower concentrations (10 mgL^{-1}); however, at higher concentration of foreign ions (100 $mg\ L^{-1}$), adsorption of Hg(II) ions was significantly decreased in the presence of these cations, indicating true competition between Hg(II) and other ions for the adsorption sites (Table T6 of supporting information ESI†).

Effect of anions

The effects of anions (i.e. PO_4^{3-}, NO_3^-, SO_4^{2-}, Cl^-) on Hg(II) ion interference were studied by addition of the potassium and sodium salt of these anions to the Hg(II) ion solutions (10 $mg\ L^{-1}$) with a concentration of 100 $mg\ L^{-1}$ of foreign anions; the results are listed in Table T6 of the supporting information (ESI†). These anions can act as ligands to form different Hg(II) ion species in aqueous solution. Results show that the efficiency of Hg(II) adsorption was not affected by the presence of PO_4^{3-}, NO_3^-, or SO_4^{2-}. On the other hand, the presence of Cl^- had a significant effect on the adsorption of Hg(II), which was concentration-dependent.[46] The interference studies show that an increase in the concentration of nitrate, phosphate, or sulphate do not affect Hg(II) uptake, while the presence of chloride leads to a drop in the sorption, which is decreased by more than 90% at 100 $mg\ L^{-1}$; lower concentrations of these anions have a small influence on Hg(II) uptake.

Comparison of adsorption behaviour based on literature data

The L-cystine-functionalised EGO adsorbent was compared in terms of adsorption capacity with some recently reported adsorbents. It is apparent that, in terms of adsorption capacity, the proposed sorbent compares favourably with other adsorbents and its adsorption capacity is quite high compared to other adsorbents (Table 1).[57-63]

Conclusion

The prospective application of L-cystine-functionalised EGO for Hg(II) adsorption has been illustrated in this work. The L-cystine amino group was involved in covalent interaction with the surface hydroxyl and carboxyl groups onto the surface of EGO. The adsorption of Hg(II) correlated with the Langmuir isotherm, maximum adsorption capacity was found to be 79.36 mg g^{-1}, and Hg(II) adsorption kinetics processes reached their equilibrium state within 45 mins, which is faster than most other graphene-based adsorbents. The thermodynamically favourable adsorption process is driven by negative enthalpy and entropy changes, respectively. The method could be scaled up to a large sample volume; as low as 10 ppb of Hg(II) could be effectively adsorbed in the column. Regeneration and stability of adsorbent for 4 repetitive cycles is yet another benefit to this interesting adsorbent material; there is considerable change in the adsorption of Hg(II) from aqueous phase in the presence of various cations and anions. The L-cystine-functionalized EGO adsorbent has carved a niche among the various other graphene-based adsorbents for adsorption of Hg(II).

Acknowledgments

The authors greatly acknowledge the Ministry of Science and Technology (MOST) of Republic of China for the research grant under contract No:100-2113-M-110-002-MY3. We also thank MOST-102-2811-M 110-039 for the post-doctoral grant.

References

1.Y. Li and C.Y. Wu, *Environ. Sci. Technol.*, 2006, **40,** 6444–6448.

2. P. Miretzky and A. F. Cirelli, *J. Hazard. Mater.,* 2009, **167,** 10–23.

3. H.Y. Jeong, B. Klaue, J. D. Blum and K.F. Hayes, *Environ. Sci. Technol.,* 2007, **41,** 7699–7705.

4.E.P.A. National Primary Drinking Water Regulations 40 CFR Ch.I (7-1-02 ed.) *US Environmental Protection Agency (EPA),* Washington, DC, 2002. http://www.access.gpo.gov/nara/cfr/waisidx 02/40cfr141 02.html.

5. J. A. Ritter and J.P. Bibler, *Water Sci. Technol.*, 1992, **25,** 165–172.

6. R. Say, E. Birlik, Z. Erdemgil, A. Denizli and A. Ersoz, *J. Hazard. Mater.*, 2008, **150,** 560–564.

7. A. K. Geim and K. S. Novoselov, *Nat. Mater.,* 2007, **6,** 183–191.

8.Z. H. Huang, X. Zheng, W. Lv, M. Wang, Q.H. Yang and Kang, F. *Langmuir,* 2011, **27,** 7558–7562.

9.H. J. Song, L.Y. Hao, Y. F. Tian, X.G. Wan, L.C. Zhang and Y. Lv, *Chem. Plus Chem.*, 2012, **77,** 379–386.

10.X. Mi, G.B. Huang, W.S. Xie, W. Wang, Y. Liu and J.P. Gao, *Carbon,* 2012, **50,** 4856−4864.

11.W.J. Zhang, X.H. Shi, Y.X. Zhang, W. Gu, B. Li and Y.Z. Xian, *J. Mater. Chem A.*, 2013, **1,** 1745−1753.

12.M. Liu, C. Chen, J. Hu, X. Wu and X. Wang, *J. Phys. Chem C.*, 2011, **115,** 25234−25240.

13.L. Fan, C.N. Luo, M. Sun and H. Qiu, *J. Mater. Chem.*, 2012, **22,** 24577−24583.

14.P. Bhunia, G. Kim, C. Baik and H. Lee, *Chem. Commun.,* 2012, **48,** 9888−9890.

15.C. J. Madadrang, H.Y. Kim, G. Gao, N. Wang, J. Zhu, H. Feng, M. Gorring, M. L, Kasner and S. Hou, *ACS Appl. Mater. Interfaces* 2012, **4,** 1186−1193.

16.Y. B. Sun, C. L. Chen, X. L. Tan, D. Shao, J. Li, G. Zhao, S. Yang and Q. Wang, *Dalton Trans.*, 2012, **41,** 13388−13394.

17.A. Santhana Krishna Kumar and N. Rajesh, *RSC Adv.*, 2013, **3,** 2697-2709.

18.J. Bao, Y. Fu and Z.H. Bao, *Nanoscale Res. Lett.,* 2013, **8,** 486-492.

19.W. Gao, M. Majumder, L.B. Alemany, T.N. Narayanan, M. A. Ibarra, B.K. Pradhan, and P.M. Ajayan, *ACS Appl. Mater. Interfaces,* 2011, **3,** 1821–1826.

20.V. Chandra and K.S. Kim, *Chem. Commun.*, 2011, **47,** 942−944.

21.X. Gong, Y. Bi, Y. Zhao, G. Liu and W. Y. Teoh, *RSC Adv.,* 2014, **4,** 24653–24657.

22. K. Chen, G. Lu, J. Chang, S. Mao, K. Yu, S. Cui and J. Chen, *Anal. Chem.,* 2012, **84,** 4057−4062.

23.S.Muralikrishna, K. Sureshkumar, T. S. Varley, D. H. Nagaraju and T. Ramakrishnappa, *Anal. Methods,* 2014, **6,** 8698–8705.

24.D. C. Marcano, D.V. Kosynkin, J.M. Berlin, A. Sinitskii, Z.Z. Sun, A. Slesarev, L.B. Alemany, W. Lu and J. M. Tour, *ACS Nano,* 2010, **4,** 4806–4814.

25.W.S. Hummers and R.E. Offeman, *J.Am.Chem. Soc.*, 1958, **80,** 1339-1341.

26.J. H. Zhu, Y. Li , Y. Chen, J. Wang, B. Zhang , J. J. Zhang, W. J. Blau, *Carbon* **2011, 49,** 1900-1905.

27.Y. Liu, Y. Li and X.P. Yan, *Adv. Funct. Mater.,* 2008, **18,** 1536–1543.

28.Y. Fu, J. Wang, Q. Liu and H. Zeng, *Carbon,* 2014, **77,** 710 – 721.

29.G. Zhao, J. Li, X. Ren, C. Chen and X. Wang, *Environ. Sci. Technol.,* 2011, **45,** 10454–10462.

30.J. Chen, B. Yao, C. Li and G. Shi, *Carbon* 2013, **64,** 225-229.

31. H.Y. Huang, R.T. Yang, D. Chinn and C. L. Munson, *Ind. Eng. Chem. Res.,* 2003, **42,** 2427–2433.

32. W.M. Davis, C. L. Eriekson, C.T. Johnston, J. J. Delfino and J.E. Porter, *Chemosphere,* 1999, **38,** 2913–2928.

33. G. Ovejero, J.L. Sotelo, M.D. Romero, A. Rodrıguez, M. A. Ocana, G. Rodriguez and J. Garcia, *Ind. Eng. Chem. Res.,* 2006, **45,** 2206–2212.

34. S. Goyanes, G.R. Rubiolo, A. Salazar, A. Jimeno, M.A. Corcuera and I. Mondragon, *Diamond Relat. Mater*., 2007, **16,** 412–17.

35. M.A. Hamon, H. Hui, P. Bhowmik, H.M.E. Itkis and R.C. Haddon, *Appl. Phys. A.* 2002, **74,** 333–338.

36. A. Hamza, A.S. Bashammakh, A.A. Al-Sibaai, H. M. Al-Saidi and M. S. El-Shahawi, *J. Hazard. Mater.*, 2010, **178,** 287–292.

37. L. Fan, C. Luo, X. Li, F. Lu, H. Qiu and M. Sun, *J .Hazard. Mater.,* 2012, **215–216,** 272– 79.

38. K. Nakamoto, *Infrared and raman spectra of inorganic and co-ordination compounds,* Wiley, New York, Third edn, 1978.

39. J. C. Feo and A. J. Aller, *J. Anal. At .Spectrom.,* 2001, **16,** 146-51.

40. T. S. Sreeprasad, S.M. Maliyekkal, K. P. Lisha and T. Pradeep, *J. Hazard. Mater.,* 2011, **186,** 921–931.

41. P.N. Lisboa-Filho, V.R. Mastelaro, W.H. Schreiner, S.H. Messaddeq, M.S. Li, Y. Messaddeq, P. Hammer, S. J. L. Ribeiro, P. Parent and C. Laffon, *Solid State Ionics.,* 2005, **176,** 1403–1409.

42. S. Ravi and M. Selvaraj, *Dalton Trans.,* 2014, **43,** 5299–5308.

43.R. S. Vieira, M.L.M. Oliveira, E. Guibal, E.R. Castellon and M. M. Beppu, *Colloids and Surfaces A: Physicochem. Eng. Aspects.,* 2011, **374,** 108–114.

44.S. Kushwaha, B. Sreedhar and P. Padmaja, *J. Chem .Eng. Data,* 2010, **55,** 4691–4698.

45.L. Jin and R. Bai, *Langmuir,* 2002, **18,** 9765-9770.

46.A. Arencibia, J. Aguado and J. M. Arsuaga, *Appl. Surface Sci.,* 2010, **256,** 5453–5457.

47.S.F. Hou, S.J. Su, M. L. Kasner, P. Shah, K. Patel and C. J. Madarang, *Chem. Phys. Lett.,* 2010, **501,** 68-74.

48.M. Madhava Rao, D.K. Ramana, K. Seshaiah, M.C. Wang and S.W.C. Chien, *J. Hazard. Mater.*, 2009, **166,** 1006–1013.

49.C.J. Daughney, S. D. Silciliano, A.N. Rencz, D. Lean and D. *Environ. Sci. Technol.,* 2002, **36,** 1546–1553.

50.M. Puanngam and F. Unob, *J. Hazard. Mater.,* 2008, **154,** 578–587.

51.I. Langmuir, *J. Am. Chem. Soc.,* 1918, **40,** 1361–1403.

52.H.M.F. Freundlich, *Z. Phys.Chem.,* 1906, **57,** 385-470.

53.S. Lagergren, *K. Sven Vetenskapsakad. Handl.,* 1898, **24,** 1-39.

54.Y.S. Ho, *J. Hazard. Mater.,* 2006, **136,** 681–689.

55.X.S. Wang, Y. Zhou, Y. Jiang and C. Sun, *J. Hazard. Mater.,* 2008, **157,** 374-385.

56.W.J.Weber and J.C. Morris, *J. Sanit. Eng. Div. Am. Soc. Civ. Eng.,* 1963, **89,** 31-60.

57.X. Guo, B. Du, Q. Wei. J. Yang, L. Hu, L. Yan and W. Xu, *J. Hazard. Mater.,* 2014, **278,** 211–220.

58.N.M. Bandaru, N. Reta, H. Dalal, A.V. Ellis and J. Joseph Shapter and N. H. Voelcker, *J. Hazard. Mater.,* 2013, **261,** 534– 541.

59.C. Zhang, J. Sui, J. Li, Y. Tang and W. Cai, *Chem. Eng. J.* 2012, **210,** 45–52.

60. T. Ninomiya, K. Oshita, M. Oshima and S. Motomizu, *Bunseki Kagaku.* 2003, **52**, 811–817.

61. Z. Yang, L. Zhuang and G. Tan, *J. Appl. Polym. Sci.* 2002, **85,** 530–535.

62. N. Dias Filho, W. Polito and Y. Gushikem, *Talanta,* 1995, **42,** 1031–1036.

63. A. Khan, F. Mahmood, M.Y. Khokhar and S. Ahmed, *React. Funct. Polym.*, 2006, **66,** 1014–1020.

Figure Captions

Fig. 1 Raman spectrum of (A) graphite (B) EGO

Fig. 2 Powder XRD pattern of (A) graphite (B) EGO

Fig. 3 ^{13}CPMAS-NMR spectrum of EGO

Fig. 4 UV spectrum of EGO

Fig. 5 FT-IR spectrum of (A) graphite (B) EGO (C) $SOCl_2$ functionalized- EGO (D) L-cystine functionalized- EGO adsorbent (E) after adsorption of Hg(II) onto L-cystine-EGO (F) L-cystine functionalized- EGO adsorbent (G) after adsorption of Hg(II) onto the adsorbent.

Fig. 6 X-ray photoelectron spectroscopy (A) total survey scan (B) carbon 1s spectrum. (C) nitrogen1s spectrum (D) mercury spectrum. (E) oxygen spectrum (F) sulphur spectrum.

Fig. 7A Illustration of interaction between L-cystine and EGO

Fig. 7B Illustration of interaction between EGO, L- cystine and Hg(II).

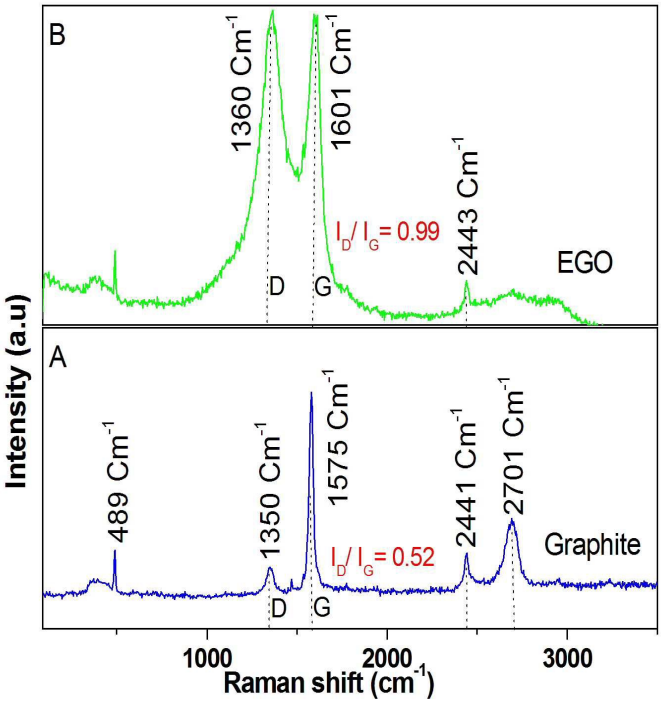

Fig. 1.

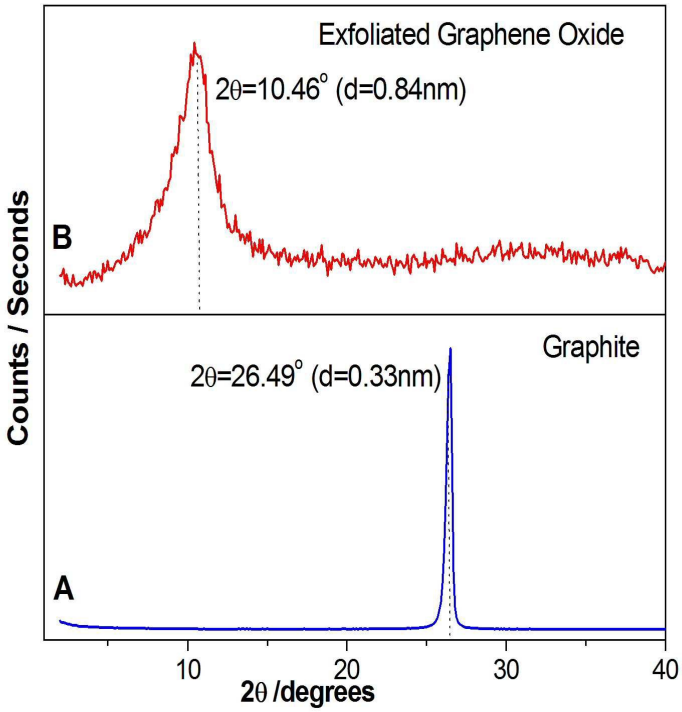

Fig. 2.

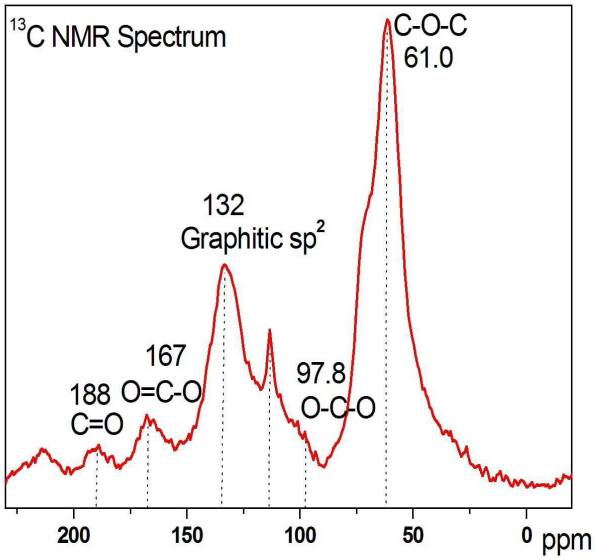

Fig. 3.

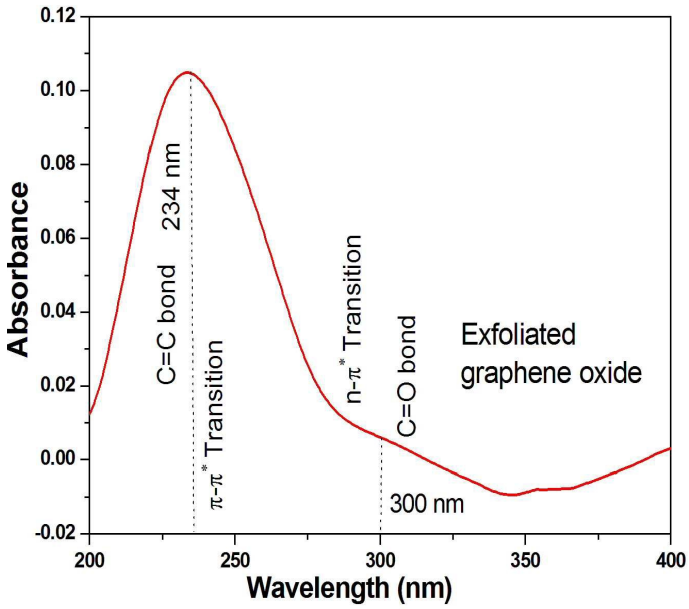

Fig. 4. .

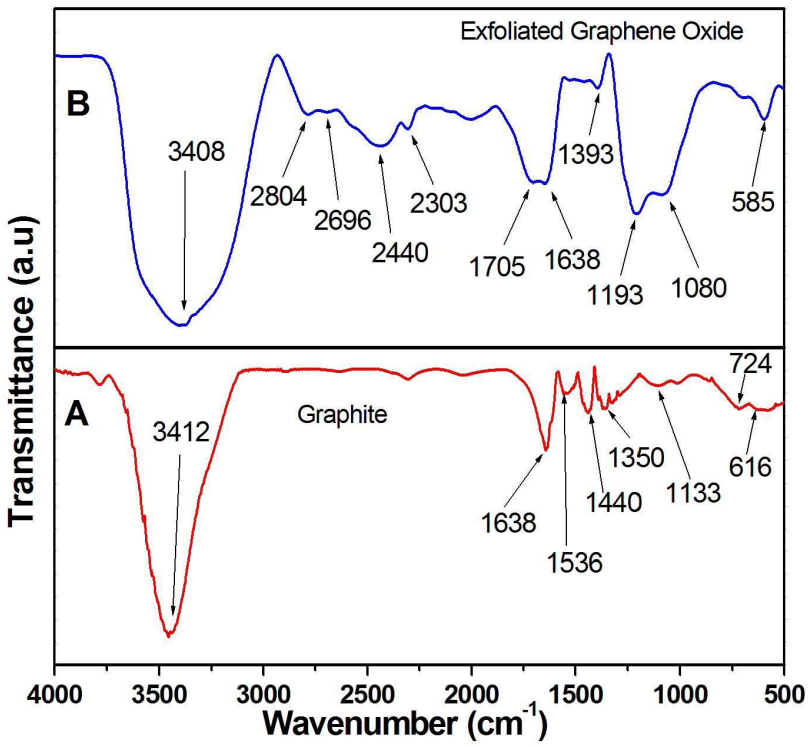

Fig. 5.

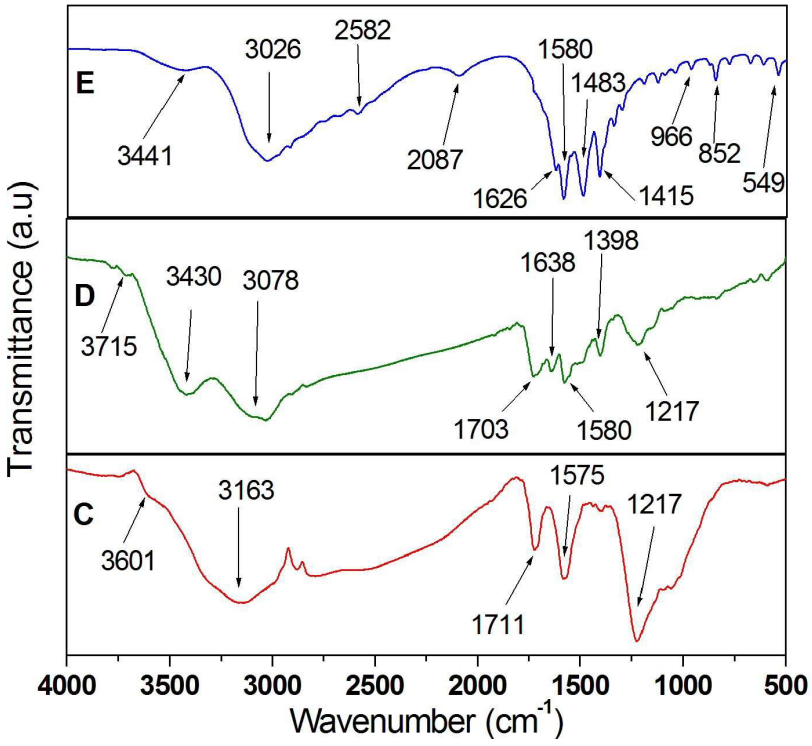

Fig. 5.

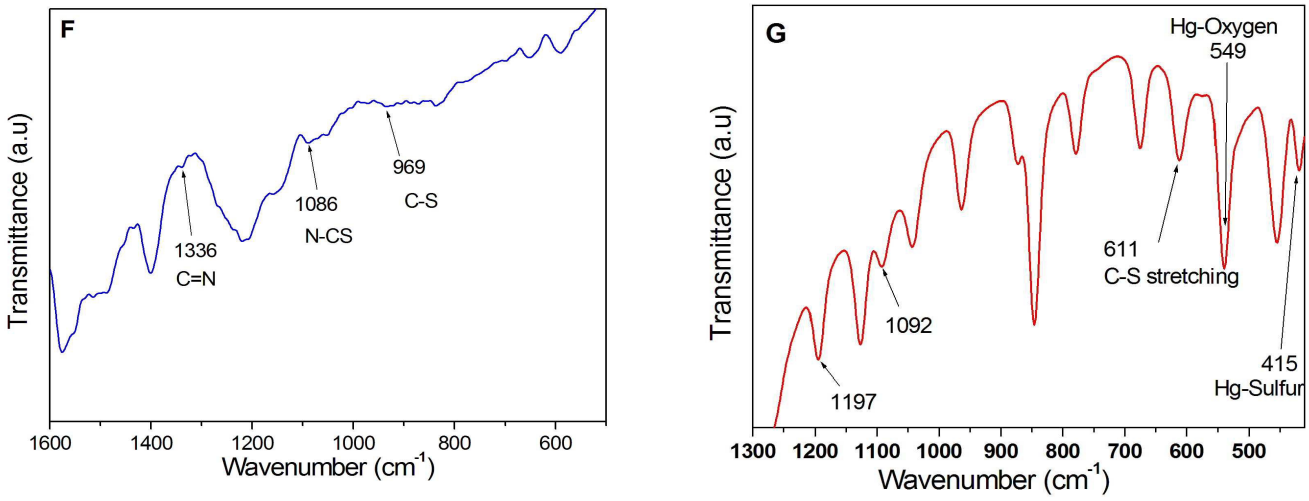

Fig. 5.

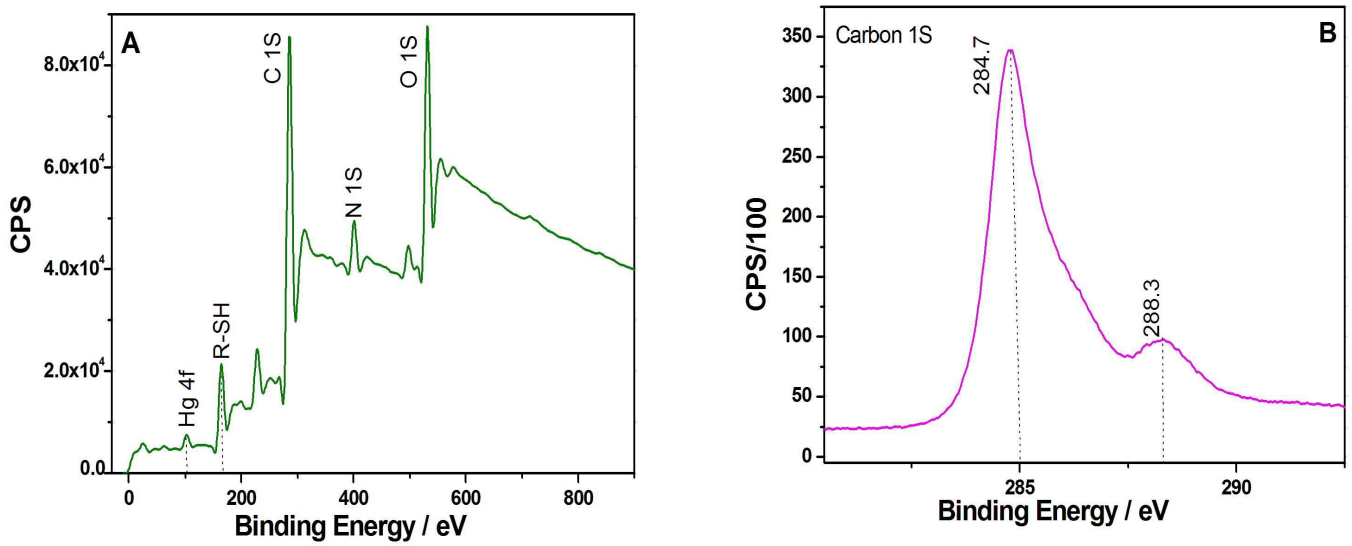

Fig. 6.

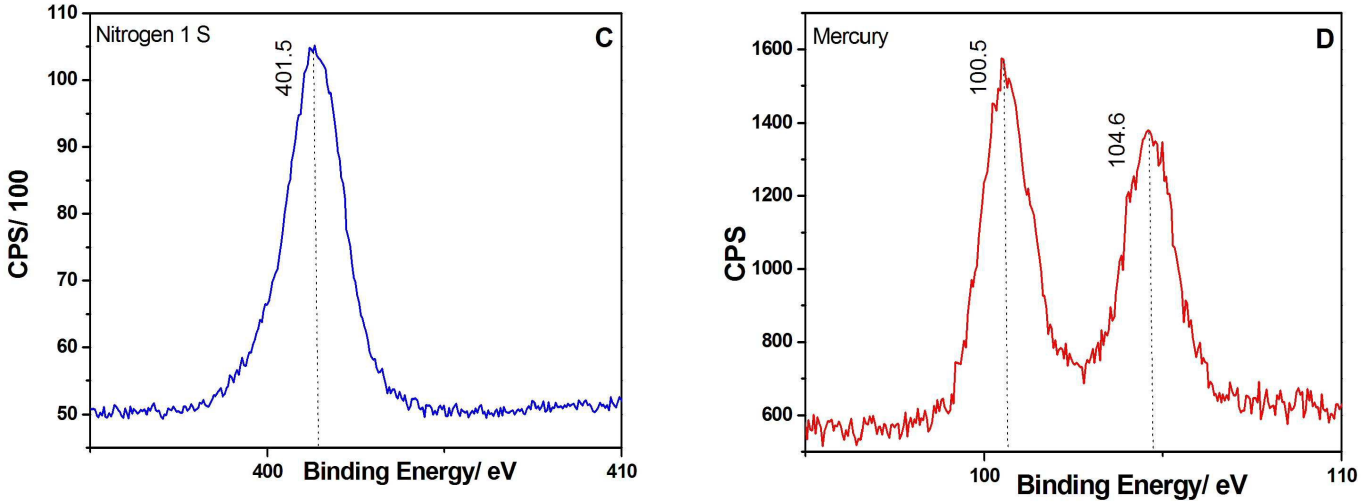

Fig. 6

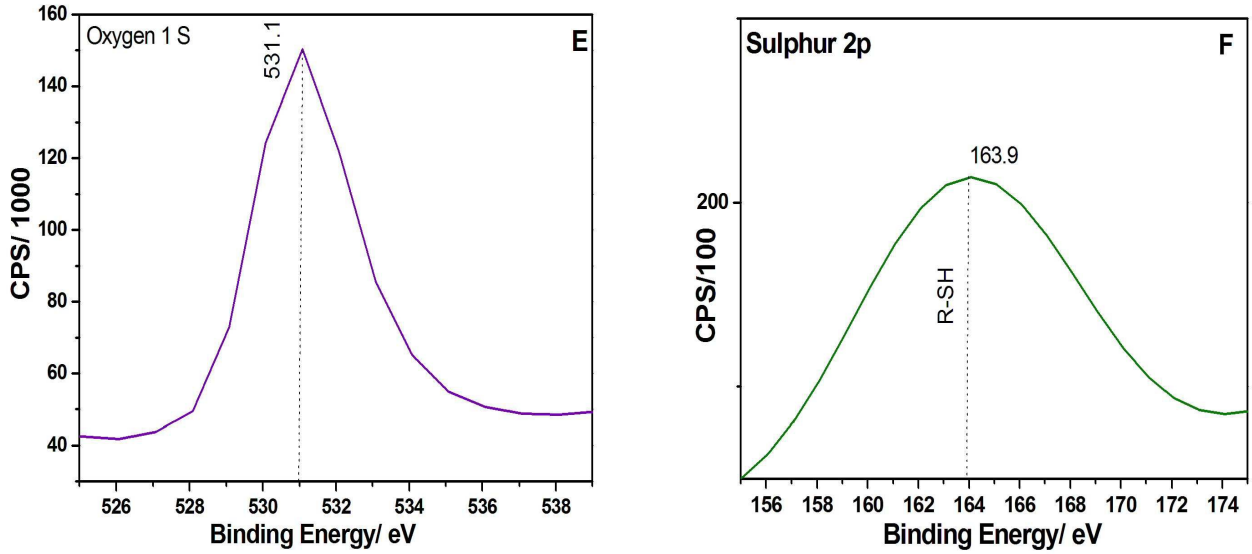

Fig. 6

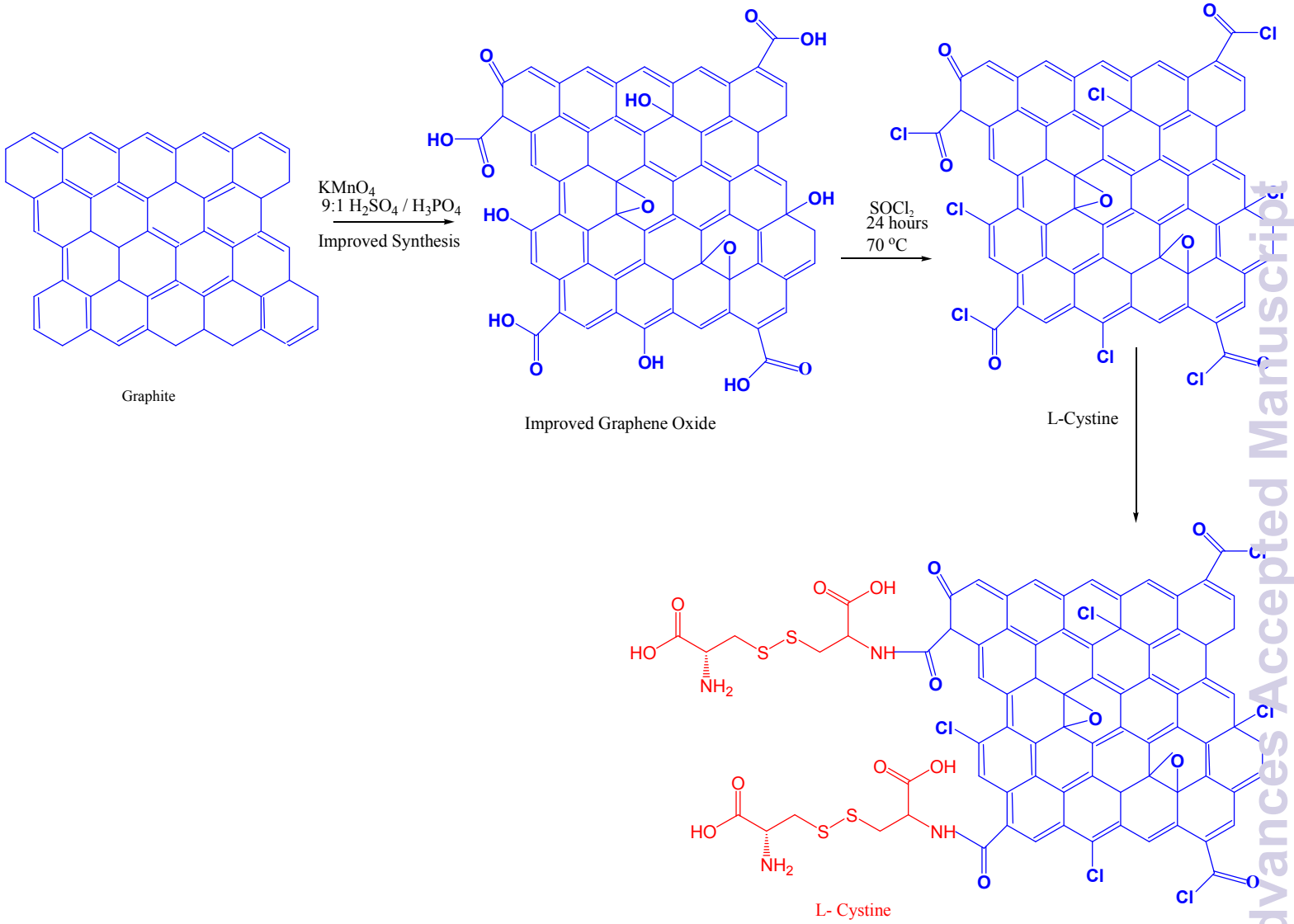

Fig. 7A

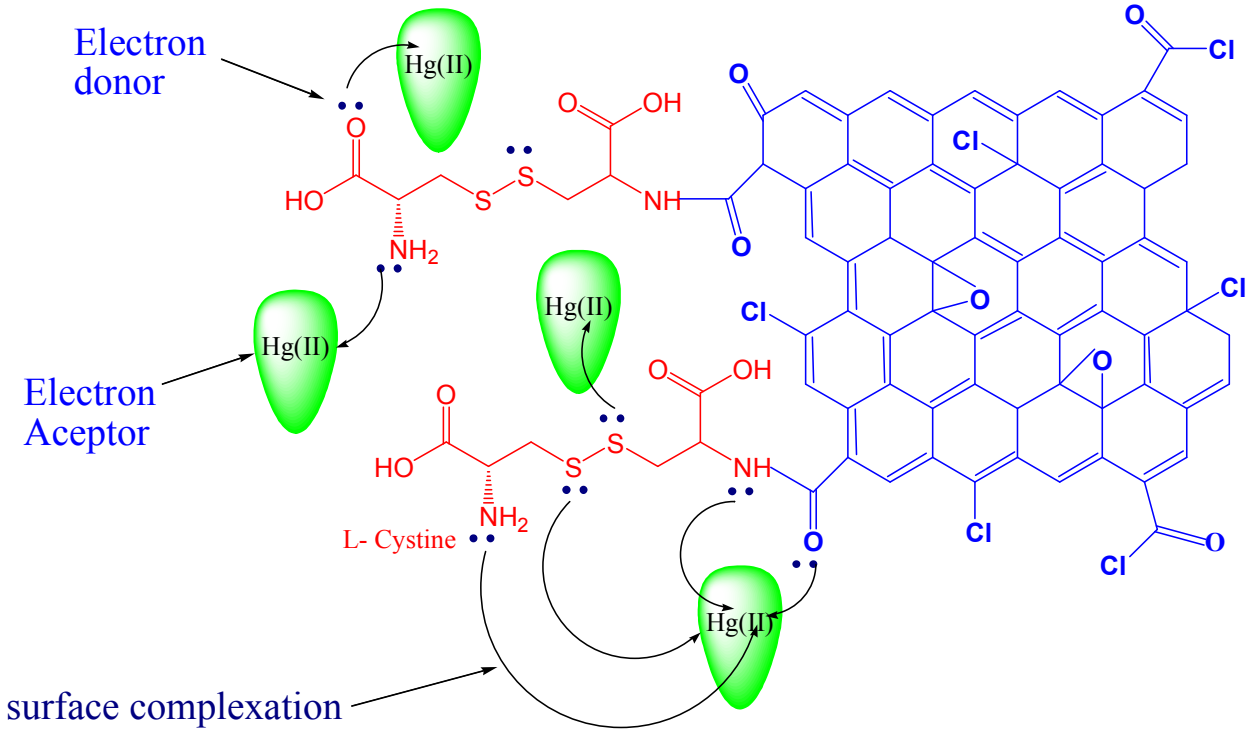

Fig. 7B

Table 1 Comparison of adsorption capacity against with other adsorbents

SI. No	Adsorbent material	Adsorption capacity (mg g^{-1})	References
1	Amino functionalized magnetic graphenes composite	23.03	57
2	Thiol derivatized single wall carbon nanotubes	39.8	58
3	3-Mercaptopropyltriethoxysilane (MPTS)-CNTs/ Fe_3O_4 nano composites.	63.65	59
4	Diethio carbamate cross-linked chitosan resin	24.07	60
5	Dihydroxy azacrown ether cross-linked chitosan (CCTS-AE)	22.1	61
6	2-Mercaptobenzothiazole treated clay	2.71	62
7	1,5 -Diphenylcarbazide immobilised sol- gel silica	29.0	63
8	Unmodified graphite	12.4	Present work
9	L-cystine functionalized EGO	79.36	Present work

Abstract

A facile and novel method for removal of Hg(II), based on the appealing interaction between exfoliated graphene oxide (EGO), L-cystine, and Hg(II), is reported in this paper. A thiol functional group facilitated the interaction with Hg(II), resulting in an efficient adsorption. The abundant oxygen-containing functional groups on the surfaces of graphene oxide (GO) play an important role in Hg(II) sorption. Characterization of the adsorbent was performed usingvarious characterization techniques, such as cross polarization magic angle spinning nuclear magnetic resonance, Raman spectroscopy, x-ray photoelectron spectroscopy, Powder-X-ray diffraction, Fourier transform infrared spectroscopy, scanning electron microscope and energy-dispersive x-ray analysis.

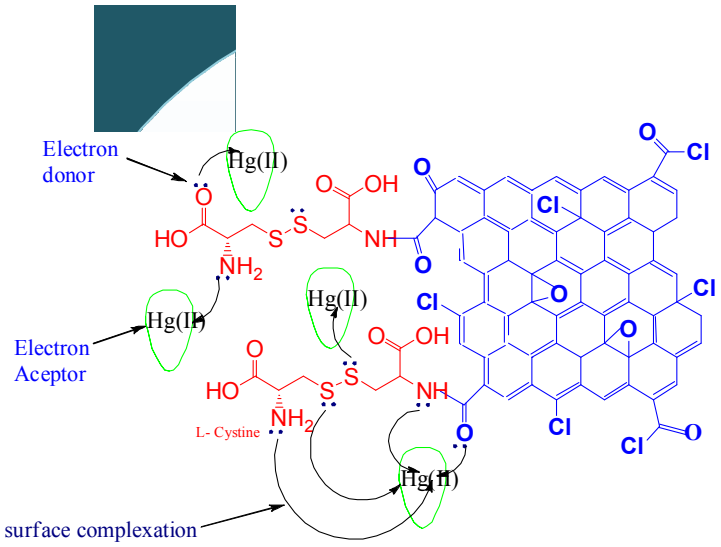

The capability of inductively-coupled plasma mass spectrometry for Hg(II) adsorption was extensively studied under different optimal parameters and the adsorption isotherm values clearly fit with the Langmuir isotherm plot; maximum adsorption capacity was 79.36 mg g^{-1}, augmented by the thermodynamically favourable adsorption process. Second-order kinetics

of the adsorption process were validated by the experimental data. Regeneration of the adsorbent was accomplished using thiourea and the potential of this novel adsorbent material was utilized in Hg(II) adsorption.

Table of contents entry:

Hg(II) adsorption involves, L-cystine bears amino group (-NH_2) could interact with GO hydroxyl and carboxyl groups through covalent bond interaction